Synthesis of Carbon Nanostructures by CVD Method

Krzysztof Koziol, Bojan Obrad Boskovic, and Noorhana Yahya

Abstract The field of nanotechnology continues to develop. Carbon based materials with different structure and dimensions become increasingly important in the field. Carbon nanotubes (CNTs) are particularly promising due to their anisotropic extraordinary electrical, thermal and mechanical properties that have captured the imagination of researchers worldwide. However, the complexity involved in synthesis of nanotubes in a predictable manner has held back the development of real-world carbon nanotube based applications. In this chapter the structure and synthesis methods will be discussed of CNTs and other forms of nanostructures of carbons. Furthermore, their structuring into macroscopic assemblies, like mats and fibres will be presented as it has important role in future industrial applications of these materials.

1 Introduction to Carbon Nanomaterials

In 1985 chemists created a new allotrope of carbon [1] by heating graphite to very high temperatures. They named the allotrope buckminsterfullerene, after American architect Richard Buckminster Fuller. The buckminsterfullerene is a molecule

K. Koziol (✉)
Department of Materials Science and Metallurgy, University of Cambridge, Pembroke Street, Cambridge, CB2 3QZ, UK
e-mail: kk292@cam.ac.uk

B.O. Boskovic
Cambridge Nanomaterials Technology Ltd, 14 Orchard Way, Cambourne Cambridge CB23 5BN, UK
e-mail: Bojan.Boskovic@cnt-ltd.co.uk

N. Yahya
Fundamental and Applied Sciences Department, Universiti Teknologi PETRONAS, Bandar Seri Iskandar, 31750 Tronoh, Perak Malaysia
e-mail: noorhana_yahya@petronas.com.my

N. Yahya (ed.), *Carbon and Oxide Nanostructures,* Adv Struct Mater 5,
DOI 10.1007/8611_2010_12,
Published online: 13 July 2010

consisting of 60 carbon atoms only (with a molecular formula of C_{60}). The molecules are shaped like tiny soccer balls (therefore sometimes referred to as buckyballs), with an atom at each point where the lines on a soccer ball would normally meet. The 60 carbon atoms bond in 20 six-membered rings and 12 five-membered rings. The discovery revolutionised the carbon field as researchers became interested in this new allotropic form of carbon. The carbon field expanded again in 1991 with Iijima's report on the observation of carbon nanotubes [2], an elongated version of buckminsterfullerenes. Carbon nanotubes, in particular, attract attention of hundreds of research groups around the world (Fig. 1) and their research still continues to grow.

The history of carbon nanotubes is much longer than 2 decades. In the 1950s and 1970s at least two groups synthesised and characterised carbon based nanotubes, but their discoveries went largely unnoticed [3, 4]. The field of carbon nanotubes has grown considerably with new, controllable production routes being developed, unusual properties predicted and measured, and many intriguing applications suggested.

The basic structure of a carbon nanotube is a hollow cylindrical tube of graphitic carbon capped by fullerene hemispheres with nanometer size diameters and macroscopic size lengths. The nanotubes may consist of one to hundreds of concentric graphitic shells of carbons. According to Saito et al. [5] the inter-sheet distance in multi-sheet nanotube is 0.344 nm. It is close to the distance between two layers in graphite, which equals to 0.335 nm [6]. The carbon network of each shell can be directly related to the hexagonal lattice of an individual layer of graphite. Nanotubes made of one hollow graphitic shell are called single wall nanotubes (SWNTs) and have diameters typically 0.6–3 nm. Nanotubes made of two or more concentric shells are called multi-walled nanotubes (MWNTs) [7] (shown in Fig. 2). In reality

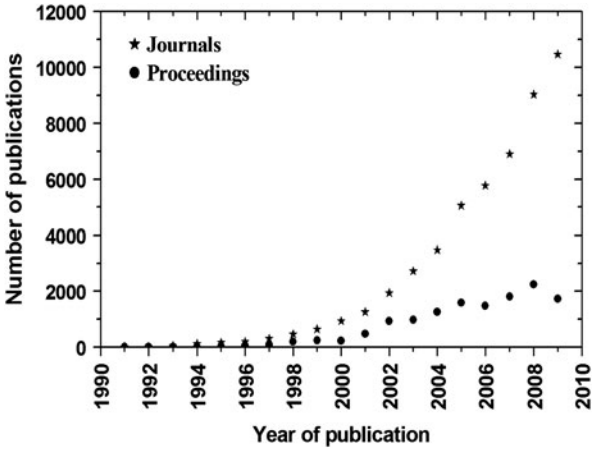

Fig. 1 Number of papers and proceedings on nanotubes per year.
Source: ISI (Institute for Scientific Information) Web of Knowledge. In the search window a term of "nanotub*" was used

multi-walled nanotubes have different lattice orientations (described with chiral vectors and angles) and defect concentration.

2 Structure of Carbon

There are several allotropes of carbon known in nature. The allotropes of carbon differ in the way the atoms bond with each other and arrange themselves into a structure (as shown in Fig. 3). As the structures of allotropes vary, they also have different physical and chemical properties [8].

In the most commonly used form, *graphite*, atoms of carbon form planar layers (graphene layers). Each layer is made up of rings containing six carbon atoms. The

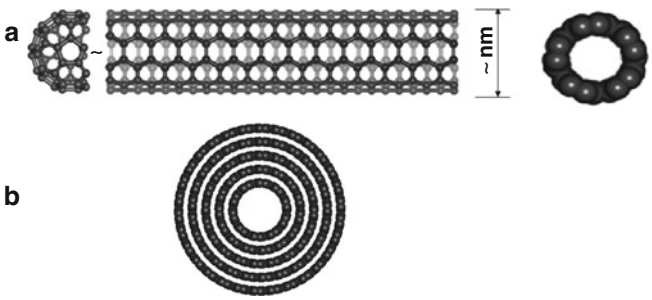

Fig. 2 Examples of ideal, defect-free nanotube structures: (**a**) side view & end on view of a single wall carbon nanotube, (**b**) end on view of a multi-walled carbon nanotube

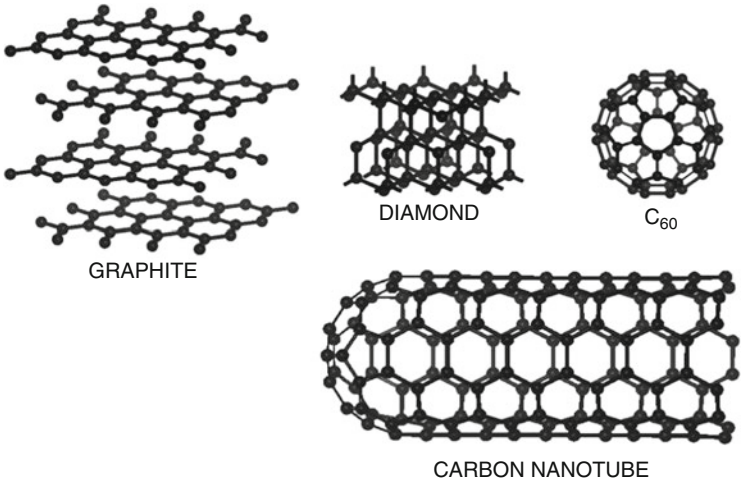

Fig. 3 Three main naturally occurring allotropes of carbon: graphite, diamond and fullerene

rings are linked to each other in a hexagonal structure. Each atom has three sigma bonds (with an angle of 120° between any two of the bonds) and belongs to three neighbouring rings. The fourth electron of each atom becomes part of an extensive π bond structure. Graphite conducts electricity due to the electrons in the π bond structure, which can move around throughout the graphite. Bonds between atoms within a graphene layer are strong, but the forces between the layers are weak, van der Waals forces [9]. The graphene layers can slip past each other, a property of graphite used in lubrication. Although graphite occur naturally, most commercial graphite is produced by treating petroleum coke, a black tar residue remaining after the refinement of crude oil, in an oxygen-free oven. Naturally existing graphite occurs in two forms, alpha (hexagonal) and beta (rhombohedral). These two forms have identical physical properties but different crystal structures. The alpha form can be converted to the beta by mechanical treatment, and the beta form reverts to the alpha on heating it above 1,000°C. All artificially produced graphite is of the alpha type.

Diamond, is one of the hardest substances known and naturally occurring form of carbon. In diamond structure, each carbon atom bonds tetrahedrally to four other carbon atoms to form a three-dimensional lattice. The shared electron pairs are held tightly in sigma bonds between adjacent atoms. Pure diamond is an electrical insulator. Due to its hardness, it is used in industrial cutting tools. The naturally occurring diamond is typically used for jewellery. However most commercial quality diamonds are artificially produced from graphite by applying extremely high pressure (more than 100,000 times the atmospheric pressure) and temperature (about 3,000°C). High temperatures break the strong bonds in graphite so that the atoms can rearrange themselves into a diamond lattice [10].

There are also amorphous forms of carbon containing varying proportions of sp^2 and sp^3 bonded carbon atoms. *Amorphous carbon* is formed when a material containing carbon is burned without enough oxygen for it to burn completely. This black soot is known as lampblack, gas black or channel black [10] and may, in fact, contain other elemental impurities. Amorphous carbon is not generally considered a third allotrope because its structure is poorly defined.

Fullerenes (buckyballs and carbon nanotubes) can be considered as a closed, zero and one dimensional carbon structure. They are the only allotrope of carbon existing in the pure form (without hydrogen terminations). Treated with hydrostatic pressure (at a level of 25 GPa) they can be converted into a hard and transparent form of amorphous carbon [11]. In comparison to atomistic crystals of graphite or diamond, fullerenes form molecular crystals. Due to the high aspect ratio of carbon nanotubes, the quasi-one-dimensional structure, and the graphite-like arrangement of the carbon atoms in the shells, nanotubes exhibit very broad range of unique properties. The properties of nanotubes can change depending on the different kinds of nanotube (defined by the diameter, length, and chiral angle) and quality (defined by defect concentration). Large increases in strength, toughness, superior electrical/thermal properties and their combination, are potential benefits of using nanotubes as the filler material in polymer-based composites as compared to traditional carbon, glass or metal fibres.

3 Synthesis Methods of Carbon Nanotubes

There is a huge demand for quality nanotubes both as research materials and for large scale industrial applications. The main problem with the currently available nanotubes is the heterogeneity of the sample, in terms of dimensions, chiral angles and purity. The nanotubes examined by Iijima in 1991 were synthesized by arc-discharge method [2], but since then several other production methods have been developed. A group led by Smalley [12] has used oven laser evaporation to produce carbon vapour, with nanotubes again observed in the condensed soot. Both arc-discharge and laser ablation techniques have the advantage of producing high quality nanotubes but at the same time relatively high amount of impurities (around 30%). Unfortunately, evaporation of carbon atoms from solid targets at temperatures above 3,000°C is neither economical and nor convenient. Synthesised CNTs may also be entangled, hindering purification steps and further application of the samples. Baker and co-workers [13, 14] demonstrated in early seventies growth of nanotubes, described at that time as carbonaceous deposits, from decomposition of acetylene. In 1976 Endo and co-workers [15–18] have also shown that CNTs can be synthesised by pyrolysis of benzene, followed by subsequent heat treatment.

Currently, the common method widely accepted in the synthesis of nanotubes, due to its simplicity and low cost, is the chemical vapour deposition (CVD) method. This method was originally developed in the 1960s and 1970s and has been successfully used in the production of carbon fibres and carbon nanofibres for more than 20 years [19–25]. Using this method, CNTs are produced from the carbon containing source (usually gaseous form) as it decomposes at elevated temperature and passes over a transition metal catalyst (typically Fe, Co or Ni) [26, 27]. A high yield of nanotubes can be achieved by this method, but the nanotubes are more structurally defective than those produced by arc or laser evaporation methods. There are several advantages of the CVD method, which make it preferred to other available synthesis methods. Firstly, the product tends to be purer (far fewer impurities in the form of nanoparticles of graphite or metal). Secondly, the growth occurs at a lower temperature (550–1,000°C) [26, 27], making the process both cheaper and more accessible for lab applications. Finally, the metal catalyst can be held on a substrate, which can lead to the growth of aligned nanotubes in a desired direction with respect to the substrate.

There are two basic mechanisms proposed for the growth of nanotubes by CVD method related to substrate bound catalyst (shown in Fig. 4), which are now widely recognised [9, 13, 14].

Top carbon diffusion through catalytic particle (tip growth model).

The decomposition of the carbon source on the exposed surface of the metal catalyst results in the formation of hydrogen and carbon species. The carbon dissolves in the particle and diffuses through it until it precipitates at the end in the form of graphene filaments. The catalytic particle sits always on the top of the growing nanotube.

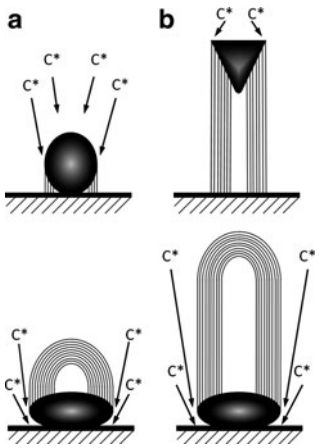

Fig. 4 Schematic diagram representing top carbon diffusion (*upper row*) and bottom carbon diffusion (*lower row*) growth mechanisms. (**a**) Pyrolysis of the hydrocarbon gas into carbon species which then dissolve in the catalyst metal particle, (**b**) precipitation of carbon in form of carbon filament

Bottom carbon diffusion through catalytic particle (base growth model).
In this model, the catalytic particle stays on the growth substrate. The carbon species dissolve in the particle and diffuses through it until they precipitate on top of the metal particle in the form of graphene filaments. The carbon diffusion parameter depends on the dimensions of the particles, the characteristics of the metal used as a catalyst, the temperature and the hydrocarbons and gases involved in the process.

When the substrate-catalyst interaction is strong, a CNT grows up with the catalyst particle rooted at its base (base growth model). When the substrate-catalyst interaction is weak, the catalyst particle is lifted up by the growing nanotube and continues to promote CNT growth at its tip (tip growth model) [23]. Formation of SWNTs or MWNTs is governed by the size of the catalyst particle. If the particle size is a few nanometers, SWNTs form, whereas particles a few tens of nanometers wide favour MWNTs formation.

The growth mechanism suggested above is quite similar to the one proposed for the vapour grown carbon fibres (VGCF), again dating 20 years back (shown in Fig. 4). Growth of these fibres occurs by a dehydrogenation reaction of a hydrocarbon gas in several steps. In this mechanism, pyrolysis of the hydrocarbon gas occurs on the surface of the catalyst particle, releasing hydrogen gas and carbon, the later dissolving into the catalyst. The dissolved carbon then diffuses through the catalyst particle and is precipitated at the trailing edge of the particle. This step possibly relies on the presence of a temperature gradient across the particle, which is often created by the exothermic nature of the hydrocarbon decomposition. This gradient causes carbon to be precipitated at the cooler trailing edge of the catalyst particle, and therefore causing the elongation of the fibre. Below is a brief summary of three main methods, by which nanotubes are produced: arc-discharge, laser ablation and chemical vapour deposition (CVD).

3.1 Arc-Discharge

The arc-discharge method is the one by which CNTs were produced by Iijima [2]. CNTs can be synthesized in the arc-discharge AC/DC system (Fig. 5). DC provides higher yields of CNTs, which are deposited on the cathode. One important condition of stabilization of arc-discharge is maintaining a constant distance between the graphite electrodes, of around 1 mm [28]. Grams scale synthesis of MWNTs by arc discharge has been achieved in He gas [29, 30]. When a graphite rod containing a metal catalyst (Fe, Co, etc.) is used as the anode with a pure graphite cathode, single-walled carbon nanotubes (SWNTs) are generated in the form of soot [31, 32].

It was found that presence of hydrogen gas in the growth region gives the optimum synthesis of MWNTs with high crystallinity (having regular graphene sheets at an interlayer spacing of 0.34 nm) and few coexisting carbon nanoparticles [2, 33–39]. In contrast, fullerenes could not be produced in gas atmosphere which included hydrogen atoms, essential difference between CNT and fullerene production [40].

3.2 Laser Ablation

The laser vaporization method was developed for fullerene and CNT production by Smalley's group [41]. First used for fullerene synthesis [1] and further applied to produce CNTs [42] in 1996, especially SWNTs. The synthesis system consists of a furnace, quartz reactor tube and laser beam source (Fig. 6). It can also consist of a reactor chamber and a laser source. A laser beam (typically a YAG or CO_2 laser) is focused onto the graphite rod target located inside the reactor tube. The target is vaporized in high-temperature argon buffer gas and carried to the copper collector cooled down with coater. The deposit is rich in SWNTs and MWNTs (Fig. 7a, b). The method has several advantages, such as high-quality SWNT production,

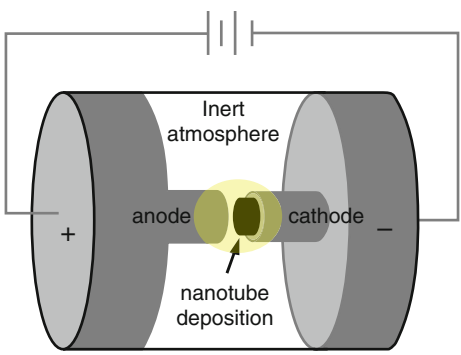

Fig. 5 Schematic diagram of the arc discharge apparatus

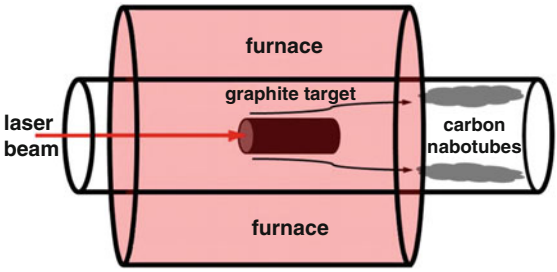

Fig. 6 Schematic diagram of the laser ablation method

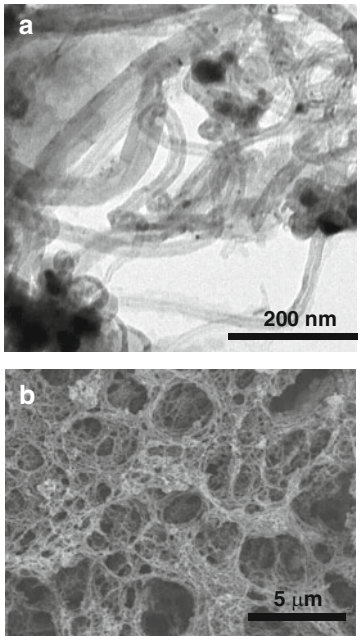

Fig. 7 (**a**) Transmission electron microscopy (TEM) image of CNTs (**b**) Scanning electron microscopy (SEM) image of carbon nanotube web structures. Both images show CNTs produced by pulsed laser ablation method (Nd:YAG laser with 532 nm wavelength was employed in this work)

diameter control, investigation of growth dynamics, and the production of new materials. High-quality SWNTs with minimal defects and contaminants, such as amorphous carbon and catalytic metals, can be synthesized using the laser-furnace method followed by suitable purification processes [43–45].

The laser has sufficiently high energy to vaporise the graphite target at the atomic level, which is then used as the material for synthesis of SWNTs [46–48]. SWNT diameter can be controlled by changing the furnace temperature, catalytic metals, and flow rate [47, 49, 50]. Raising the furnace temperature results in SWNTs with larger diameters [49]. Depending on the choice of the catalytic metals, the diameter of the SWNTs can either be increased or reduced [50, 51].

3.3 Thermal Catalytic Chemical Vapour Deposition

This method involves pyrolysis of hydrocarbons (acetylene, ethylene, propylene, methane, benzene, toluene etc.) or other carbon feedstock (polymers, carbon monoxide) diluted in the stream of inert gas in the furnace system over the surface of metal catalysts [15, 52–55]. The evaporation of a solid hydrocarbon can be conveniently achieved in another furnace at low temperature before the main, high-temperature reaction furnace [56–61]. The catalyst material may be solid, liquid, or gas and can be placed inside the furnace or fed in continuously from outside. Decomposed carbon species dissolve in the metal nanoparticles but, due to a finite solubility of carbon in the metallic particles, supersaturation will be reached followed by carbon precipitation out in the form of a fullerene dome extending into a carbon cylinder [19, 62]. Typical temperature range for the synthesis is 500–1,200°C at atmospheric pressure [6, 52].

Typical system used in the thermal CVD method of making carbon nanotubes, with horizontally positioned reaction tube is shown in Fig. 8.

The CVD method allows CNT growth in a variety of forms, such as powder, thin or thick films, aligned or entangled, straight or coiled, or even a desired architecture of nanotubes at predefined sites on a patterned substrate. It also offers better control over growth parameters in comparison to other synthesis methods. The three main parameters for CNT growth in CVD are the atmosphere, carbon source, catalyst, and growth temperature. Low-temperature (600–900°C) yields MWNTs, whereas a higher temperature (900–1,200°C) reaction favours SWNTs growth [63–68].

The most commonly used catalysts for CNT growth are the transition metals (Fe, Co, Ni) from sources like organometallocenes (ferrocene, cobaltocene, nickelocene), nitrates and others [69, 70]. A correlation was found between the size of catalyst particles and the nanotube diameter. Hence, metal nanoparticles of controlled size can be used to grow CNTs of controlled diameter [71].

The CVD process has been scaled up onto a large scale commercially, especially for MWNTs [72–74]. Smalley's lab developed a mass production of SWNTs by the so-called high pressure carbon monoxide (HiPco) technique [75]. Currently also

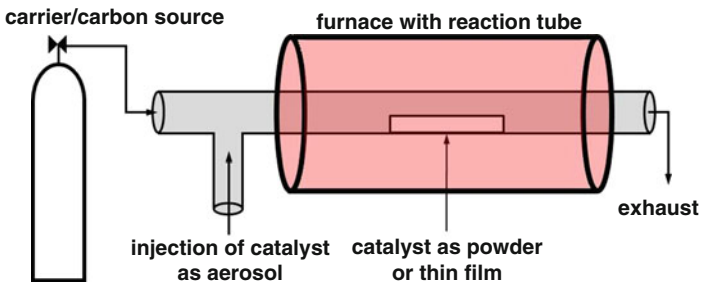

Fig. 8 Schematic design of a thermal CVD system with a tube furnace

kilograms scale of MWNTs per hour can be produced [76, 77] even with the control over the diameter of nanotubes.

3.3.1 Synthesis of Aligned Carbon Nanotubes

Generally, it is hard to grow aligned CNTs (SWNTs or MWNTs) by arc discharge, although partial alignment of the nanotubes can be achieved by convection [78] or directed arc plasma [79]. The CVD method is ideally suited to grow aligned CNTs on desired substrates for specific applications. Li et al. [80] have grown dense MWNTs arrays on iron-impregnated mesoporous silica prepared by a sol-gel process, Terrones et al. [81] have produced CNTs on Co-coated quartz substrates, while Pan et al. [82] have reported the growth of aligned CNTs of more than 2 mm in length over mesoporous substrates from acetylene. Depending on the preferred application highly aligned nanotubes were synthesised with different catalysts [83] or on different substrates [73, 84–86]. Using the CVD method it is also possible to grow aligned nanotubes in a desired direction with respect to the growth substrate. It was also found that not all materials can be active in the growth of aligned nanotubes. Metal, graphite or silicon used in the process would not yield any nanotubes. Substrates made of silica or alumina would generate nanotubes. Additionally it has been demonstrated that the growth of CNTs depends on the thickness of the oxide layer on silicon wafer surface [84]. Below 6 nm no detectable growth of the nanotubes was observed. Above 50 nm thick oxide layer gives saturation and growth dependence only on CVD time. However between 6 and 50 nm the growth of aligned nanotubes seems to be depended on both CVD time and SiO_2 layer thickness.

It has been shown that full control over the length of CNTs could be achieved and aligned, densely pack nanotubes produced (as in Fig. 9). The inhibition of CNTs growth at low SiO_2 thickness is explained by partial deactivation of catalyst

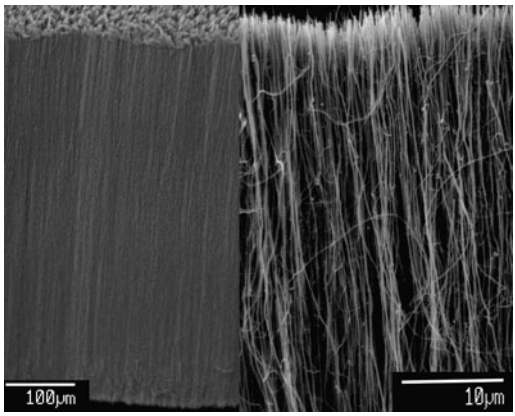

Fig. 9 Electron microscope images of highly aligned carbon nanotube car pets, at low and high magnifications

particles due to their reaction with the silicon substrate. Iron from ferrocene (source of metal) diffuses through SiO_2 layers thinner than ~5 nm and reacts with the silicon substrate, leading to formation of $FeSi_2$ and $FeSiO_4$, neither of which catalyses CNTs growth. The layer of SiO_2 with thickness above 5 nm is sufficient enough to keep the active metal particle and promote the suitable metal structure conducive to CNTs growth.

3.3.2 Synthesis of Nitrogen Doped Nanotubes

Shortly after the synthesis of carbon nanotubes, a quest of substitution of carbon atoms in the graphene network with heteroatoms such as boron, nitrogen, sulphur, phosphor and silicon begun. The intensive work on heteroatomic doping was aiming to alter some of the important properties of nanotubes, including electrical (electron density and semiconducting character), mechanical (improvement of Young's modulus), and chemical (change of reactivity, creation of catalytically active centres etc.) [87].

There are three basic ways that nitrogen can be incorporated into the graphene CNTs structure. (1) Substitution, where N is coordinated to three C atoms in sp^2 like fashion, which induces sharp localized states above the Fermi level associated with the injection of additional electrons into the structure. (2) Pyridine-like substitution, where N is arranged around a vacancy, since the valency of the nitrogen can be satisfied by two sp^2 bonds, a delocalised p-orbital, and a lone pair in the remaining sp^2 orbital, pointing at the vacancy. (3) Chemical adsorption of N_2 molecules.

Nitrogen contains one electron more than carbon; therefore, substitutional doping of nitrogen within graphene will n-dope the structure, enhancing the number of electronic states at the Fermi level depending on the location and concentration of dopant. Hernandez et al. calculated the mechanical properties of nitrogen and boron doped nanotubes [88, 89], demonstrating that high concentrations of N within SWNTs lower the Young's modulus. Nevertheless, the Young's modulus values still remain on the order of 0.5–0.8 TPa. This behaviour has been experimentally confirmed in pristine and N-doped MWNTs [90]. Unfortunately, the Young's modulus for pristine and N-doped MWNTs were 0.8–1 TPa and ~30 GPa, respectively. The decrease in mechanical strength of N-doped nanotubes could be explained by the nitrogen induced defects due to the relatively high N concentration (2–5%) within the tubes. If the N concentration is below 0.5%, it is expected that the mechanical properties will not be substantially altered [91].

Results from other theoretical studies demonstrated that relative position of nitrogen and carbon affects not only electronic properties but also their thermodynamic stability [92].

Studies using ab initio density functional theory have shown that the nitrogen substitution into zigzag and armchair SWNTs can cause a junction of separate tubes by the formation of covalent bonds [93]. If two neighbouring tubes have their nitrogen impurities facing one another, inter-tube covalent bonds could potentially be formed. If the density of inter-tube bond is high enough, a highly packed bundle

of interlinked single-walled nanotubes can form, substantially enhancing the mechanical properties.

There are two main routes used to synthesis the N-CNTs: (1) direct delivery of heteroatoms with the carbon source stream, during the growth of the nanotubes (2) substitution of carbon atoms by heating the nitrogen containing compound with CNTs. The most common is the first route.

Similar methods as in the case of pure carbon nanotubes are used in the synthesis of nitrogen-doped nanotubes. In the arc-discharge method the atmosphere surrounding electrodes must contain nitrogen. Depending on the percentage of nitrogen in the growth atmosphere, different nitrogen doping levels have been recorded [94]. The doping level was up to 14 %wt (as determined by XPS) when 50 %vol of atmosphere was substituted by nitrogen. The resulting N-CNTs had diameters of about 20 nm and were coated with a thick layer of amorphous carbon. Computational calculations showed that incorporation of nitrogen atoms lead to distortion in graphite plane [94].

Arc experiments using pure graphite electrodes in an NH_3 atmosphere indicated that it was difficult to produce N-doped SWNTs and MWNTs, possibly because N_2 molecules are easily created and do not react with carbon [91]. N-doped SWNTs could be produced by arcing composite anodes containing graphite, melamine, Ni, and Y [95].

The laser ablation method was not fully explored in the synthesis of doped nanotubes. In 1997, Zhang et al. [96] reported that sandwich-like C-B-N nanotubes could be produced by laser vaporisation of graphite-BN targets. However it is likely that a large N content will result in the inhibition of SWNT growth. More energetic lasers were proposed in order to generate N- or B-doped SWNTs.

In the CVD method the usual approach relied on the pyrolysis of hydrocarbons or other carbon feedstock with the addition of a nitrogen source (e.g. nitrogen, ammonia, amines, nitriles) diluted in the stream of the inert gas in the furnace system over the surface of metallic catalyst particles (such as Fe, Co or Ni). The catalyst can be provided with the stream of starting materials or deposited directly onto the growth substrates. The differences between the reported processes arise from the application of different nitrogen sources, catalysts and pressures. Depending on the conditions and parameters of the synthesis, different quality of growth products was reported. It has been suggested that only small concentrations of nitrogen (below 15%) can be introduced into MWNTs [97]. The results demonstrated that it is extremely difficult to generate crystalline and highly ordered structures containing large concentrations of N within the hexagonal carbon network. The doped nanotubes with low N concentrations have been subsequently generated via pyrolysis of pyridine and methylpyrimidine [98]. Unfortunately, these nanotubes are easily oxidized in air. The degree of perfection within graphene sheets changes rapidly with different N concentration used. Keskar et al. prepared isolated N-doped SWNTs from thermal decomposition of a xylene-acetonitrile mixture over nanosized iron catalyst particles. The N dopant concentration was controlled by the amount of acetonitrile in the mixture [99].

Liang et al. reported that using ferrocene and ethylenediamine as a source of catalyst and nitrogen resulted in increased of the diameter of nanotubes with increasing growth temperature. The majority of the material containing nitrogen was formed as MWNTs in the bamboo-like structure. The N-doping level also was dependent on growth temperature. With increasing temperature from 780 to 1,080°C the amount of nitrogen decreased from 24 to 18 %wt. N-doped CNTs grown at lower temperatures have shown much higher degree of disorder and higher N-incorporation [100].Wang et al. shown that the longer the time of synthesis, the higher the length and diameter of nanotubes produced, which was suggested to correlate with the grain size of catalyst particles (the longer the growth time, the larger the iron catalyst particles). The bamboo-like morphology of nanotubes was again observed. The doping levels of nitrogen were estimated by EELS at 9% [101]. Lee et al. used acetylene and ammonia in argon and varied the growth temperature from 750 to 950°C. When increasing the amount of nitrogen source an increase in doping level from 2.8 to 6.6 %wt was observed by elemental analysis [102]. Again bamboo-shaped morphology of nanotubes was present. Additionally using ammonia as a source of nitrogen caused decrease in the growth rate of N-CNTs.

Two different bamboo-type morphologies of nanotubes were reported by Glerup et al. One type with a very frequent, regular compartments and another with irregular structure with fewer, longer and uneven compartments. Chemical analysis showed presence of molecular nitrogen trapped inside the nanotubes. It is not clear if the nitrogen is homogeneously distributed along the length of the nanotube or whether it is segregated into regions with higher and lower concentrations [103]. Jang et al. demonstrated that an increase in the flow rate of nitrogen yielded in more defective graphene sheets and higher doping levels [104]. Lee et al. used acetylene and ammonia as a source for synthesis and presented microscopy and spectroscopy evidence revealing consistently that as the nitrogen source increases the degree of crystallinity (nanotube structure perfection) decreases. Again the N-content varied in the range 2–6 %wt depending on the ammonia flow rate. It was found that the higher the nitrogen incorporation the more curved and thicker bamboo-like compartments appear [105].

In 2005, Koziol et al. demonstrated completely different outcome, to what was already reported, by using specific nitrogen precursors in CVD synthesis of nanotubes. In this case hydrocarbon feedstock containing diazine, aromatic compound with nitrogen, at a critical level, was injected to the reactor at 760°C. The nanotubes, which they synthesised, were multiwalled but found to be extremely straight and had unprecedented degrees of internal order [106]. Furthermore, electron diffraction patterns from individual nanotubes, revealed that all of the walls had the same chiral angle, which is not possible in concentric cylindrical nanotubes, due to a geometric constrains but possible in conical nanotubes (Fig. 10). The adjacent nanotube walls in these nanotubes were in crystallographic register with one another, with ABAB stacking sequences of layers [106]. Finally, and most importantly, the chiral angles seen in electron diffraction patterns were of the simple achiral forms and nanotubes were consistently either armchair or zigzag, as seen in Fig. 10 (middle and left) [106]. Very low conical angle was measured in these nanotubes, between 0.5° and 5° and

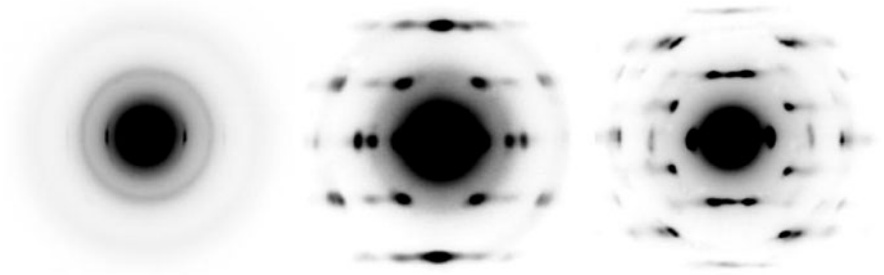

Fig. 10 Electron diffraction patterns from individual multiwalled nanotubes. Standard mix chirality (*left*), armchair (*middle*), zigzag (*right*) [106]

nitrogen was detected in two forms, as substitution in the lattice and as N_2 gas in the core of every tube [107–109]. Higher diazine concentrations in the feedstock seemed to allow the formation of shallower cones [108].

3.4 Plasma Enhanced Chemical Vapour Deposition

Carbon nanotubes and nanofibres can be synthesised using plasma enhanced CVD (PECVD) where the hydrocarbon gas is in an ionised state over the transition metal catalyst (nickel, iron, cobalt, etc.). The carbon nanotube and nanofibre aligned growth perpendicular to the substrate can be achieved using the electrical self-bias field from plasma (Fig. 11). PECVD systems are characterised primarily by the plasma energy sources used, and the most commonly used include: hot filament PECVD, direct current PECVD, radio-frequency PECVD, microwave PECVD.

Hot filament PECVD uses thermal energy for plasma creation and has been used successfully for carbon nanotube production by Ren and co-workers [110]. Microwave PECVD, widely used for the preparation of diamond films, has also been successfully used in the production of carbon nanotubes and nanofibres [111–115]. Synthesis of vertically aligned CNTs and CNFs requires electric field normal to the substrate, and dc PECVD is the most suitable method to achieve this [116, 117]. Inductively coupled plasma PECVD [118, 119] and radio frequency PECVD [120, 121] methods have also been used successfully for carbon nanotubes and nanofibres synthesis. Ren et al. in 1998 [110] reported first successful growth of large-scale well-aligned carbon nanofibres on nickel foils and nickel-coated glass at temperatures below 666°C. Bower et al. [114] have grown well-aligned carbon nanotubes using microwave PECVD with additional radio frequency graphite heater. They found that switching the plasma source off effectively turns the alignment mechanism off leading to the thermal growth of curly nanotubes. Merkulov et al. [116] reported synthesis of vertically aligned CNFs on patterned catalyst using dc PECVD. The catalyst patterns were fabricated using conventional electron beam lithography. The shape of CNFs depends on how much growth occurs at the tip by catalysis and now much by

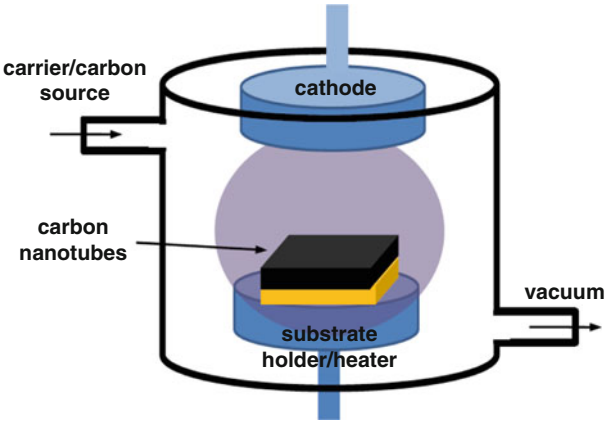

Fig. 11 Schematic design of a parallel plate PECVD system

deposition of a-C from the plasma along the sidewalls [122]. This ratio is controlled by the catalyst activity and by the balance of deposition and etching of a-C. The balance between deposition and etching depends on the plasma and the etchant (NH_3) and hydrocarbon gas (C_2H_2). This balance has been studied by Merkulov et al. [116] and Teo et al. [123].

In plasma enhanced CVD systems, plasma energy sources substitute for the thermal energy in a furnace, and provide the energy required for decomposition of hydrocarbon feedstock and allow growth of carbon nanostructures at much lower temperatures.

The PECVD method allows growth of carbon nanotubes and nanofibres at low temperatures suitable for use of temperature sensitive substrates. A radio frequency PECVD carbon nanofibres synthesis at room temperature has been reported by Boskovic et al. [121]. A room temperature growth of carbon nanofibers using PECVD was subsequently demonstrated by Minea et al. [124]. Using dc PECVD Hofmann et al. [125] demonstrated synthesis of aligned carbon nanofibres at temperatures as low as 120 °C and on plastic substrates [126].

Although MWCNT and nanofibers synthesis have been achieved through PECVD at low temperature [121], SWCNT synthesis still remains largely a high temperature process (800–1,200°C) produced in arc-discharge, laser ablation, or tube furnace. Cantoro et al. [127] recently reported thermal CVD synthesis of SWCNT at temperature as low as 350°C in very low pressure (10^{-3}–10^{-2} mbar) of pure acetylene in a cold-walled system.

4 Other Forms of Carbon Nanostructures

Besides the carbon nanotubes, other interesting carbon nanostructures have been sythesised using CVD. The carbon nanohorns, carbon nanowalls and graphene have received considerable interests. The radial packing of single-walled tubular carbon

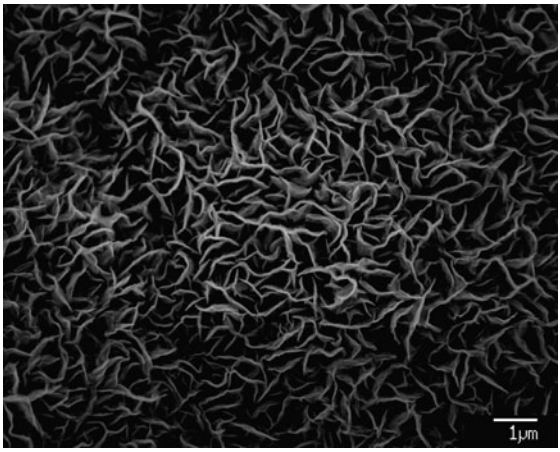

Fig. 12 Carbon nanowalls grown in the MW PECVD as described by Chuang et al. [138, 139]

nanohorns resembles a dahlia flower. Iijima et al. [128] described the growth mechanism of carbon nanohorns: In a high energy and low diffusion rate condition carbon species forms graphene sheets, and collide to form horn structures as predicted by tight-binding molecular-dynamics simulations [129].

Carbon nanowalls (CNWs) are networks of vertically aligned graphitic walls. They share similar morphology with other carbon nanomaterials such as carbon nanoflakes [36, 130, 131], and nanosheets [132, 133], and nanoflowers [134]. Two-dimensional CNWs, first reported by Wu et al. [135], are promising materials for a number of applications, and have been demonstrated as an efficient material for backlights of liquid crystal displays by field emission in the form of a nanodiamond/carbon nanowalls composite [136], also as high-brightness lamps based on CNW-coated nickel wires [137]. High surface area also makes CNW suitable for electrochemical applications, such as batteries and fuel cells.

Carbon nanowalls was first reported as a surface-bound material, by Wu et al. [135], synthesized in an attempt to produce CNT in PECVD environment. Chuang et al. [138, 139] reported the first successful synthesis non-surface bound free-standing macroscopic structure of CNW aggregates by microwave PECVD in various ammonia/acetylene gas mixtures (Fig. 12). This process is extremely efficient, and neither catalyst nor a flat substrate was needed. Carbon nanowall aggregates extrude from plasma sites induced by a growth stage and grow freely into three-dimensional space. The overall length can reach centimeters in 10 min of deposition time.

4.1 Carbon Nanotube Fibres

Significant attention was devoted into development of methods for manufacture of carbon nanotube based fibres. CNTs were used as the main constituent material in

fibres or in combination with a polymeric matrix. In each case the aim was to take advantage of the spectacular axial properties of nanotubes. Carbon nanotube fibres would be an ideal system to translate the fabulous properties of individual nanotubes into real macroscopic use. One challenge in the fibre system is to achieve nanotube-nanotube bonding to get good load transfer and contact free flow of electrons. Second challenge is to find a convenient and economical way to manufacture CNT fibres.

First CNT fibre with a polymeric matrix was reported by Vigolo et al. [140]. Single wall nanotube dispersion was co-extruded with polyvinyl alcohol (PVA)/water through a long syringe into a rotating water/PVA coagulation bath. The coagulation method used produced long fibres and ribbons. The diameter of the fibres could be adjusted by changing the injection rate, flow conditions, and dimensions of the capillary tube that affect the thickness of the ribbons. Authors have demonstrated the flexibility of the carbon nanotube fibres by making knots and they showed the fiber can be curved through 360° without breaking. The elastic modulus of SWNTs fibres was an order of magnitude higher than the modulus of high-quality bucky paper.

With long-range directional order, liquid crystals have long been used as precursor solutions for spinning high performance fibres. With lengths on the order of nanometers, and typical lengths in microns, CNTs have approximately the same shape as small molecules like tobacco mosaic virus, which readily form liquid crystalline phases. Liquid crystalline behaviour in CNTs was predicted by Somoza et al. in 2001, based on a computational model using continuum-based density-functional theory [141]. Somoza analyzed the different possibilities for tailored liquid crystalline CNT phases, predicting the formation of a columnar liquid crystalline phase. However liquid crystallinity in aqueous carbon nanotube suspension was first reported by Song et al. [142]. It opened a possible route for drawing fibres from liquid crystalline suspensions of carbon nanotubes.

Davis et al. at Rice University announced realization of nematic phases of SWNTs in superacid solutions. The SWNTs were produced using their high-pressure carbon monoxide (HiPco) process [143, 144]. Up to 10 wt% of SWNTs were dispersed in a superacid solution of sulphuric acid, chlorosulfonic acid, and triflic acid. Such a high concentration represents a tenfold increase over previous dispersions of SWNTs, and is due to the protonation of the nanotubes and the formation of an electrostatic double layer of protons and counter ions [145]. This charged layer surrounding individual nanotubes both encourages solubility in water, as well as preventing aggregation due to the repulsive force felt by like-charged nanotubes. Ericson et al. used sulfuric acid to promote the alignment of SWNTs and extruded fibres consisting entirely of SWNTs [146]. The purified SWNTs were mixed with 102% sulphuric acid and the mixture was extruded through a small capillary tube into a coagulation bath after its viscosity has reached a steady state. Fibres were obtained under different conditions, such as coagulants, different dope temperatures and coagulation bath temperatures. These fibres showed good alignment, with XRD analysis showing a mosaic angle of 31° at full width at half maximum (FWHM), and Raman spectroscopy showing a Raman

ratio greater than 20:1. Additionally, fibres coagulated in water had a density that was 77% or the theoretical close packing density for 1.0 nm nanotubes. These fibres possess good mechanical properties, with a Yong's modulus of 120 ± 10 GPa and a tensile strength of 116 ± 10 MPa [146].

A simple and alternative route to spin CNT fibres directly from their lyotropic liquid crystalline phase consisting of multiwalled carbon nanotubes was shown by Zhang et al. [147]. The nanotubes were highly aligned within the fibres due to the combination of shear forces and the liquid crystalline phase. Fibres spun with carbon nanotubes and nitrogen-doped nanotubes (N-MWNTs) were both examined. High resolution transmission electron microscope shows N-MWNTs were much straighter than the MWNTs. Ethylene-glycol was used as a matrix to disperse nanotubes, with the concentrations between 1 and 3 wt%. A low power ultrasonic bath was used to assist the nanotubes dispersion process. The dispersion went from isotropic to biphasic to nematic phase with increasing concentration. The dispersions were then extruded out of the syringe through a needle with diameter less than 130 μm and transfer directly into a bath containing diethyl-ether. A syringe pump was used to control the extrusion rate of the dispersions and they were collected on a spindle outside the bath at the rate of 0.03–0.3 m/min. Young's modulus of MWNT fibres was found to be 69 ± 41 GPa. On the other hand, N-MWNT fibres had much higher stiffness of 142 ± 70 GPa, more than twice of the MWNT fibres [147]. The different mechanical properties between two types of fibres were believed to be the different interaction between individual nanotubes. The straighter N-MWNTs were thought to have less defects and a higher packing density, i.e. better interactions between the tubes. The electrical properties were measured by the two-probe method and both fibers were found to have ohmic behaviour, but N-MWNTs showed higher conductivity.

Direct spinning of CNTs into fibres is one method that can offer advantages over post-processing methods. Fewer processing steps lead to simpler and cheaper synthesis, and ease of scaling and commercialization. Jiang et al. have spun fibres directly from dense forests of MWNTs [148]. These CNT forests, grown by chemical vapour deposition (CVD), enable the continuous drawing of nanotubes due to van der Waal interactions between the nanotubes. Zhang et al. [149] introduced twist during spinning of multiwalled carbon nanotubes from nanotube forests to make multi-ply, torque-stabilized yarns. The yarn diameter was set by controlling the width of the forest sidewall that was used to generate an initial wedge-shaped ribbon and they have made singles (unplied), two-ply and four-ply MWNT yarns. The unplied yarn had diameters between 1 and 10 μm. The twist was typically 80,000 turns/m, versus 1,000 turns/m for conventional textiles (with much higher diameter). Single twisted fibres showed tensile strengths between 150 and 300 MPa. These single fibres were then spun into multi-ply yarns, with the two-ply having tensile strengths between 250 and 460 MPa. Later Zhang et al. made carbon nanotube sheets by rotating carbon nanotubes in vertically oriented nanotube arrays [150]. This method combines the dry-state spinning of nanotube yarns from forests and the introduction of twist. They demonstrated the thickness of the sheet depended on the forest size and increased with increasing the forest height. These

transparent sheets have been used for the planar sources of polarized broad-band radiation and flexible organic light-emitting diodes. Zhang et al. at Los Alamos National Laboratory demonstrated the spinning of fibres from CNT arrays of 300, 500, and 650 μm in length and they found the tensile strengths for those as-spun fibres were 0.32, 0.56, and 0.85 GPa, respectively [151]. The work indicated that the fibre strength increased with increasing CNT length.

The most direct technique for spinning of CNT fibres was developed by Windle's group at University of Cambridge. This method relies on drawing carbon nanotube fibres directly and continuously from the CVD synthesis zone of a furnace [152]. Any type of hydrocarbon can be used as a source of carbon, injected at one end of the furnace together with thiophene (used as synthesis enhancer) and organometallic precursor, typically ferrocene, which after the decomposition forms iron nanoparticles allowing the formation of CNTs. These CNTs form an aerogel in the furnace hot zone, and due to their intermolecular interactions, as "elastic smoke" can be drawn from the furnace (as shown in Fig. 13) and wound onto a rotating spool [152]. There appears to be no limit to the length of the fibres drawn, presenting a truly continuous process. The continuous spinning process relies on two critical factors. One is to have sufficient high-purity nanotubes to form an aerogel in the furnace hot zone and the other is the forcible removal of the material from reaction by continuous wind-up. Different carbon sources and furnace temperature will produce CNT fibres with varies structures and properties. The composition of the fibres, in terms of double walled or multiwalled nanotubes could be controlled by changing the reaction parameters.

Additionally, Koziol et al. developed a controlled method for continuous spinning of fibres from the CVD reactor with different nanotube orientation based on the liquid condensation and drawing from the CVD reactor [153]. The mechanical data obtained demonstrate a considerable potential of carbon nanotube assemblies in the quest for maximal mechanical performance. The strength values measured in these fibres up to 10 GPa exceed any known available high performance material.

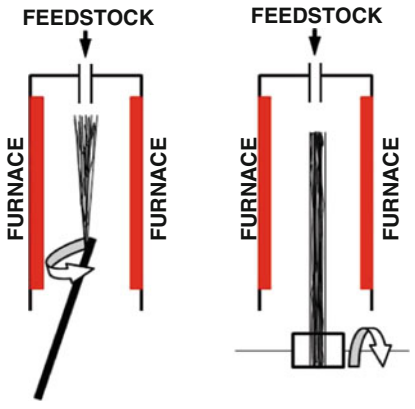

Fig. 13 Schematic of the direct aerosol spinning process (*left*); The wind-up procedure is operated outside the furnace hot zone at room temperature (*right*)

The development of continuous fibre drawing methods represents an enormous leap forward in the attempt to scale CNT properties for use in macroscopic applications. Now that researchers have realized success in spinning such fibres, attention must turn to designing processes that will provide increased tensile strength and modulus, approaching that of individual nanotubes. Better control of the underlying chemistry will allow experimentalists to fine-tune the nanotube properties, including length, axial alignment and surface functionalization.

4.2 3D Carbon-Carbon Nanomaterials

Three-dimensional (3D) nano-carbon structures that can transfer exceptional properties of carbon nanomaterials to meso- and micro-scale engineering materials are essential for development of many applications [154]. Tennent et al. [155] at Hyperion Catalysis in 1998 patented a method of preparing 3D microscopic structures by dispersing carbon fibrils (nanotubes or nanofibers) in a medium and separating them from the medium by filtration and evaporation to form a porous mat or sheet. Carbon nanotubes and nanofibers synthesized using CVD are usually in the form of a powder or a thin film on a flat substrate and direct synthesis of 3D carbon nanotube and nanofiber macroscopic structures are still challenging.

Well known engineering materials like carbon, ceramic or glass fibres could be exploited as a support for the formation of 3D nano-structures. Growth of CNTs and CNFs on the surface of carbon fibres was first reported to improve composite shear strength [156, 157] and load transfer at the fibre/matrix interface [158]. The high surface area of carbon and ceramic fibres coated with nanotubes and nanofibres is important for use in electrochemical applications [159–161]. Jo et al. [162] reported excellent field emission properties of CNTs grown on the surface of carbon fibres in carbon cloth, which could potentially be used in flat panel displays. Boskovic et al. [163] reported low temperature DC PECVD synthesis of carbon nanofibres on the surface of carbon fibres (Fig. 14) using Co colloid catalyst. It was also demonstrated that using the same Co colloid catalyst and the same PECVD method it is possible to grow carbon nanotubes and nanofibres on arbitrary micro-machined silicon three-dimensional “micro-grass” surfaces [164]. Hart et al. [164] demonstrated that conventional metal deposition techniques can be used to obtain uniform SWCNT and DWCNT film growth by atmospheric pressure thermal CVD on arbitrarily micro-structured silicon “micro-grass” surfaces, where the surfaces face the deposition source in any orientation from vertical to horizontal. These principles can be applied to grow a wide variety of nanostructures on microstructures having arbitrary 3D topography, extending the fabrication capability for hierarchically micro-structured and nano-structured substrates. Carbon fibres bundles, woven and non-woven carbon fibre cloth can be used as a three-dimensional scaffold for carbon nanotube synthesis on surface of carbon fibres and in the empty space between them. Boskovic has found [165] that when the catalyst is

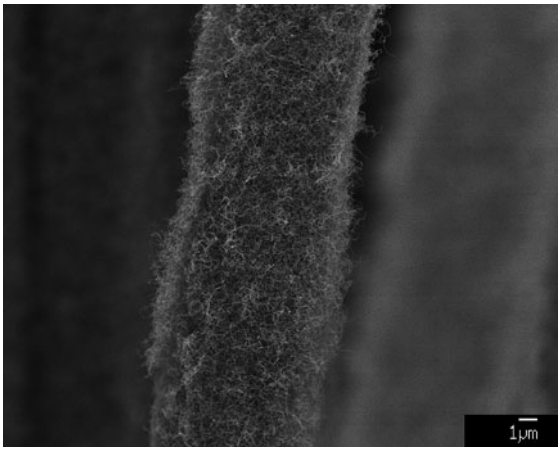

Fig. 14 Carbon nanotubes synthesised on the carbon fibre surface using thermal CVD

impregnated and dispersed within a fibrous matrix (carbon or ceramic fibre cloth or felt), rather than being left on the surface, a more efficient deposition of nanofibres and/or nanotubes results. Fine iron powder catalyst dispersed in isopropanol was impregnated within a 2.5 mm thick VCL N carbon cloth, obtained from Morgan Specialty Graphite, Fostoria, OH, USA using an ultrasonic bath. The samples were then dried producing a fibrous matrix with an impregnated finely dispersed metal powder. Carbon nanotubes and nanofibres were grown using an ethylene and hydrogen mixture at 650°C. The nanotubes/nanofibres are produced in clumps originating from the surface of the catalyst particles. The amount of produced carbon nanomaterials could be controlled using variation of catalyst loading.

Veedu et al. [166] reported that well-aligned CNTs grown perpendicular to 2D woven fabric of SiC fibres improved significantly the mechanical and thermal properties. Interlaminar fracture-toughness of the resulting 3D composite has shown an improvement of 348% compared with the base composite without CNTs. The interlaminar shear sliding fracture toughness was improved by about 54%. It is also reported that addition of carbon nanotubes has significantly improved dissipation of vibration energy under cyclic loading – damping (514%). The coefficient of thermal expansion was reduced to 38% of the original value and thermal conductivity was improved by 51%. Three-dimensional composite materials containing carbon nanotubes and carbon fibres are good candidate for many potential applications. High thermal conductivity of these materials may be of use in automotive and aerospace applications and for heat distribution or hot spot control. Recently, Boskovic patented use for aircraft brake applications [167]. The high electrical conductivity of these materials could be used for example in electronic components packaging, as gas diffusion layers in fuel cells or in electromagnetic shielding. The carbon fabric impregnated with carbon nanotubes could be used for lightweight structures and for bulletproof vests.

5 Conclusions

In this chapter we presented different carbon nanostructures but the focus was particularly on carbon nanotubes, their methods of synthesis, heteroatomic doping and exquisite properties. The processing of nanotubes and macroscopic realisation of the properties through the fabrication of fibres and 3D structures is further presented and compared.

Acknowledgement Dr Krzysztof Koziol thanks The Royal Society for financial support at the University of Cambridge.

References

1. Kroto, H.W., Heath, J.R., O'Brien, S.C., Curl, R.F., Smalley, R.E.: Nature **318**, 162–163 (1985)
2. Iijima, S.: Nature **354**, 56–58 (1991)
3. Ball, P.: Nature **414**, 142–144 (2001)
4. Radushkevich, L.V., Lukyanovich, V.M.: J. Phys. Chem. **26**, 88–95 (1952)
5. Saito, Y., Yoshikawa, T., Bandow, S., Tomita, M., Hayashi, T.: Phys. Rev. B **48**, 1907–1909 (1993)
6. Popov, V.N.: Mater. Sci. Eng. R **43**, 61–102 (2004)
7. Ebbesen, T.W.: Carbon Nanotubes: Preparation and Properties, 1st edn. CRC, Boca Raton (1997)
8. Encarta: Online Encyclopedia (2004)
9. Terrones, M.: Int. Mater. Rev. **49**, 325–377 (2004)
10. Pierson, H.O.: Handbook of Carbon, Graphite, Diamond and Fullerenes. William Andrew Publishing, Norwich (1993)
11. Moshary, F., Chen, N.H., Silvera, I.F., Brown, C.A., Dorn, H.C., Devries, M.S., Bethune, D.S.: Phys. Rev. Lett. **69**, 466–469 (1992)
12. Guo, T., Nikolaev, P., Rinzler, A.G., Tomanek, D., Colbert, D.T., Smalley, R.E.: J. Phys. Chem. **99**, 10694–10697 (1995)
13. Baker, R.T.K., Barber, M.A., Harris, P.S., Feates, F.S., Waite, R.J.: J. Catal. **26**, 51–62 (1972)
14. Baker, R.T.K., Waite, R.J.: J. Catal. **37**, 101–105 (1975)
15. Endo, M., Takeuchi, K., Igarashi, S., Kobori, K., Shiraishi, M., Kroto, H.W.: J. Phys. Chem. Solids **54**, 1841–1848 (1993)
16. Sarkar, A., Kroto, H.W., Endo, M.: Carbon **33**, 51–55 (1995)
17. Endo, M., Takeuchi, K., Kobori, K., Takahashi, K., Kroto, H.W., Sarkar, A.: Carbon **33**, 873–881 (1995)
18. Endo, M.: Chemtech **18**, 568–576 (1988)
19. Tibbetts, G.G.: J. Cryst. Growth **66**, 632–638 (1984)
20. Tibbetts, G.G.: Carbon **27**, 745–747 (1989)
21. Tibbetts, G.G.: J. Cryst. Growth **73**, 431–438 (1985)
22. Tibbetts, G.G., Devour, M.G., Rodda, E.J.: Carbon **25**, 367–375 (1987)
23. Baker, R.T.K.: Carbon **27**, 315–323 (1989)
24. Walker, P.L., Rakszawski, J.F., Imperial, G.R.: J. Phys. Chem. **63**, 133–140 (1959)
25. Dresselhaus, M.S., Dresselhaus, G., Surihara, K., Spain, I.L., Goldberg, H.A.: Graphite Fibers and Filaments. Springer, Berlin (1988)

26. Ci, L.J., Zhao, Z.G., Dai, J.B.: Carbon **43**, 883–886 (2005)
27. Dresselhaus, M.S., Dresselhaus, G., Avouris, Ph.: Springer-Verlag, Germany (2001)
28. Ebbesen, T.W.: Phys. Today **49**, 26–32 (1996)
29. Ebbesen, T.W., Ajayan, P.M.: Nature **358**, 220–222 (1992)
30. Colbert, D.T., Zhang, J., Mcclure, S.M., Nikolaev, P., Chen, Z., Hafner, J.H., Owens, D.W., Kotula, P.G., Carter, C.B., Weaver, J.H., Rinzler, A.G., Smalley, R.E.: Science **266**, 1218–1222 (1994)
31. Iijima, S., Ichihashi, T.: Nature **363**, 603–605 (1993)
32. Bethune, D.S., Kiang, C.H., Devries, M.S., Gorman, G., Savoy, R., Vazquez, J., Beyers, R.: Nature **363**, 605–607 (1993)
33. Ando, Y., Iijima, S.: Jpn. J. Appl. Phys. Part 2 **32**, L107–L109 (1993)
34. Ando, Y.: Fullerene Sci Technol **2**, 173–180 (1994)
35. Wang, M., Zhao, X.L., Ohkohchi, M., Ando, Y.: Fullerene Sci Technol **4**, 1027–1039 (1996)
36. Ando, Y., Zhao, X., Ohkohchi, M.: Carbon **35**, 153–158 (1997)
37. Zhao, X., Ohkohchi, M., Wang, M., Iijima, S., Ichihashi, T., Ando, Y.: Carbon **35**, 775–781 (1997)
38. Wang, X.K., Lin, X.W., Dravid, V.P., Ketterson, J.B., Chang, R.P.H.: Appl. Phys. Lett. **66**, 2430–2432 (1995)
39. Ando, Y., Zhao, X.L., Ohkohchi, M.: Jpn. J. Appl. Phys. Part 2 **37**, L61–L63 (1998)
40. Tai, Y., Inukai, K., Osaki, T., Tazawa, M., Murakami, J., Tanemura, S., Ando, Y.: Chem. Phys. Lett. **224**, 118–122 (1994)
41. Guo, T., Diener, M.D., Chai, Y., Alford, M.J., Haufler, R.E., Mcclure, S.M., Ohno, T., Weaver, J.H., Scuseria, G.E., Smalley, R.E.: Science **257**, 1661–1664 (1992)
42. Thess, A., Lee, R., Nikolaev, P., Dai, H.J., Petit, P., Robert, J., Xu, C., Lee, Y.H., Kim, S.G., Rinzler, A.G., Colbert, D.T., Scuseria, G.E., Tomanek, D., Fischer, J.E., Smalley, R.E.: Science **273**, 483–487 (1996)
43. Bandow, S., Rao, A.M., Williams, K.A., Thess, A., Smalley, R.E., Eklund, P.C.: J. Phys. Chem. B **101**, 8839–8842 (1997)
44. Chiang, I.W., Brinson, B.E., Huang, A.Y., Willis, P.A., Bronikowski, M.J., Margrave, J.L., Smalley, R.E., Hauge, R.H.: J. Phys. Chem. B **105**, 8297–8301 (2001)
45. Ishii, H., Kataura, H., Shiozawa, H., Yoshioka, H., Otsubo, H., Takayama, Y., Miyahara, T., Suzuki, S., Achiba, Y., Nakatake, M., Narimura, T., Higashiguchi, M., Shimada, K., Namatame, H., Taniguchi, M.: Nature **426**, 540–544 (2003)
46. Puretzky, A.A., Geohegan, D.B., Fan, X., Pennycook, S.J.: Appl. Phys. A **70**, 153–160 (2000)
47. Sen, R., Ohtsuka, Y., Ishigaki, T., Kasuya, D., Suzuki, S., Kataura, H., Achiba, Y.: Chem. Phys. Lett. **332**, 467–473 (2000)
48. Kokai, F., Takahashi, K., Yudasaka, M., Iijima, S.: J. Phys. Chem. B **104**, 6777–6784 (2000)
49. Bandow, S., Asaka, S., Saito, Y., Rao, A.M., Grigorian, L., Richter, E., Eklund, P.C.: Phys. Rev. Lett. **80**, 3779–3782 (1998)
50. Kataura, H., Kumazawa, Y., Maniwa, Y., Ohtsuka, Y., Sen, R., Suzuki, S.: Carbon **38**, 1691–1697 (2000)
51. Kataura, H., Kimura, A., Ohtsuka, Y., Suzuki, S., Maniwa, Y., Hanyu, T., Achiba, Y.: Jpn. J. Appl. Phys. Part 2 **37**, L616–L618 (1998)
52. Journet, C., Bernier, P.: Appl. Phys. A Mater. Sci. Process. **67**, 1–9 (1998)
53. Yacaman, J.M., Yoshida, M.M., Rendon, L.: Appl. Phys. Lett. **62**, 657–659 (1993)
54. Satishkumar, B.C., Govindaraj, A., Rao, C.N.R.: Chem. Phys. Lett. **307**, 158–162 (1999)
55. Hernadi, K., Fonseca, A., Nagy, J.B., Bernaerts, D., Lucas, A.A.: Carbon **34**, 1249–1257 (1996)
56. Maruyama, S., Kojima, R., Miyauchi, Y., Chiashi, S., Kohno, M.: Chem. Phys. Lett. **360**, 229–234 (2002)
57. Murakami, Y., Miyauchi, Y., Chiashi, S., Maruyama, S.: Chem. Phys. Lett. **377**, 49–54 (2003)

58. Murakami, Y., Chiashi, S., Miyauchi, Y., Hu, M.H., Ogura, M., Okubo, T., Maruyama, S.: Chem. Phys. Lett. **385**, 298–303 (2004)
59. Kumar, M., Ando, Y.: Diam. Relat. Mater. **12**, 998–1002 (2003)
60. Kumar, M., Ando, Y.: Chem. Phys. Lett. **374**, 521–526 (2003)
61. Kumar, M., Kakamu, K., Okazaki, T., Ando, Y.: Chem. Phys. Lett. **385**, 161–165 (2004)
62. Baker, R.T.K., Harris, P.S. Chemistry and physics of carbon. In: Walker, P.L., Thrower, P.A. (eds.) Dekker, New York (1978)
63. Dai, H., Rinzler, A.G., Nikolaev, P., Thess, A., Colbert, D.T., Smalley, R.E.: Chem. Phys. Lett. **260**, 471–475 (1996)
64. Cheng, H.M., Li, F., Sun, X., Brown, S.D.M., Pimenta, M.A., Marucci, A., Dreselhaus, G., Dresselhaus, M.S.: Chem. Phys. Lett. **289**, 602–610 (1998)
65. Satishkumar, B.C., Govindaraj, A., Sen, R., Rao, C.N.R.: Chem. Phys. Lett. **293**, 47–52 (1998)
66. Hafner, J.H., Bronikowski, M.J., Azamian, B.R., Nikolaev, P., Rinzler, A.G., Colbert, D.T., Smith, K.A., Smalley, R.E.: Chem. Phys. Lett. **296**, 195–202 (1998)
67. Kong, J., Cassell, A.M., Dai, H.J.: Chem. Phys. Lett. **292**, 567–574 (1998)
68. Flahaut, E., Govindaraj, A., Peigney, A., Laurent, C., Rousset, A., Rao, C.N.R.: Chem. Phys. Lett. **300**, 236–242 (1999)
69. Yudasaka, M., Kikuchi, R., Ohki, Y., Yoshimura, S.: Carbon **35**, 195–201 (1997)
70. Rao, C.N.R., Sen, R., Satishkumar, B.C., Govindaraj, A.: Chem. Commun. **15**, 1525–1526 (1998)
71. Ago, H., Komatsu, T., Ohshima, S., Kuriki, Y., Yumura, M.: Appl. Phys. Lett. **77**, 79–81 (2000)
72. Sen, R., Govindaraj, A., Rao, C.N.R.: Chem. Phys. Lett. **267**, 276–280 (1997)
73. Andrews, R., Jacques, D., Rao, A.M., Derbyshire, F., Qian, D., Fan, X., Dickey, E.C., Chen, J.: Chem. Phys. Lett. **303**, 467–474 (1999)
74. Nikolaev, P., Brownikowsky, M.J., Bradley, R.K., Rohmund, F., Colbert, D.T., Smith, K.A., Smalley, R.E.: Chem. Phys. Lett. **313**, 91–97 (1999)
75. Bronikowski, M.J., Willis, P.A., Colbert, D.T., Smith, K.A., Smalley, R.E.: J. Vac. Sci. Technol. A **19**, 1800–1805 (2001)
76. Couteau, E., Hernadi, K., Seo, J.W., Thien-Nga, L., Miko, C., Gaal, R., Forro, L.: Chem. Phys. Lett. **378**, 9–17 (2003)
77. Wang, Y., Wei, F., Luo, G.H., Yu, H., Gu, G.S.: Chem. Phys. Lett. **364**, 568–572 (2002)
78. Zhao, X., Inoue, S., Jinno, M., Suzuki, T., Ando, Y.: Chem. Phys. Lett. **373**, 266–271 (2003)
79. Huang, H., Kajiura, H., Tsutsui, S., Hirano, Y., Miyakoshi, M., Yamada, A., Ata, M.: Chem. Phys. Lett. **343**, 7–14 (2001)
80. Li, W.Z., Xie, S.S., Qian, L.X., Chang, B.H., Zou, B.S., Zhou, W.Y., Zhao, R.A., Wang, G.: Science **274**, 1701–1703 (1996)
81. Terrones, M., Grobert, N., Olivares, J., Zhang, J.P., Terrones, H., Kordatos, K., Hsu, W.K., Hare, J.P., Townsend, P.D., Prassides, K., Cheetham, A.K., Kroto, H.W., Walton, D.R.M.: Nature **388**, 52–55 (1997)
82. Pan, Z.W., Xie, S.S., Chang, B.H., Wang, C.Y., Lu, L., Liu, W., Zhou, M.Y., Li, W.Z.: Nature **394**, 631–632 (1998)
83. Li, J., Papadopoulos, C., Xu, J.M., Moskovits, M.: Appl. Phys. Lett. **75**, 367–369 (1999)
84. Cao, A.Y., Ajayan, P.M., Ramanath, G., Baskaran, R., Turner, K.: Appl. Phys. Lett. **84**, 109–111 (2004)
85. Fan, S.S., Chapline, M.G., Franklin, N.R., Tombler, T.W., Cassell, A.M., Dai, H.J.: Science **283**, 512–514 (1999)
86. Wei, B.Q., Vajtai, R., Jung, Y., Ward, J., Zhang, R., Ramanath, G., Ajayan, P.M.: Nature **416**, 495–496 (2002)
87. Zhao, M.W., Xia, Y.Y., Lewis, J.P., Zhang, R.Q.: J. Appl. Phys. **94**, 2398–2402 (2003)
88. Hernandez, E., Goze, C., Bernier, P., Rubio, A.: Phys. Rev. Lett. **80**, 4502–4505 (1998)
89. Hernandez, E., Goze, C., Bernier, P., Rubio, A.: Appl. Phys. A. Mater. **68**, 287–292 (1999)

90. Gao, R.P., Wang, Z.L., Bai, Z.G., de Heer, W.A., Dai, L.M., Gao, M.: Phys. Rev. Lett. **85**, 622–625 (2000)
91. Terrones, M., Jorio, A., Endo, M., Rao, A.M., Kim, Y.A., Hayashi, T., Terrones, H., Charlier, J.C., Dresselhaus, G., Dresselhaus, M.S.: Mater. Today **10**, 30–45 (2004)
92. Huang, Y.H., Gao, J.P., Liu, R.Z.: Synthetic Met. **113**, 251–255 (2000)
93. Nevidomskyy, A.H., Csanyi, G., Payne, M.C.: Phys. Rev. Lett. **91**, 105502 (2003)
94. Droppa, R., Hammer, P., Carvalho, A.C.M., dos Santos, M.C., Alvarez, F.: Journal of Non-Crystalline Solids **299**, 874–879 (2002). Part B
95. Glerup, M., Steinmetz, J., Samaille, D., Stephan, O., Enouz, S., Loiseau, A., Roth, S., Bernier, P.: Chem. Phys. Lett. **387**, 193–197 (2004)
96. Zhang, Y., Gu, H., Suenaga, K., Iijima, S.: Chem. Phys. Lett. **279**, 264–269 (1997)
97. Terrones, M., Hsu, W.K., Terrones, H., Zhang, J.P., Ramos, S., Hare, J.P., Castillo, R., Prassides, K., Cheetham, A.K., Kroto, H.W., Walton, D.R.M.: Chem. Phys. Lett. **259**, 568–573 (1996)
98. Sen, R., Satishkumar, B.C., Govindaraj, S., Harikumar, K.R., Renganathan, M.K., Rao, C.N. R.: J. Mater. Chem. **7**, 2335–2337 (1997)
99. Keskar, G., Rao, R., Luo, J., Hudson, J., Chen, J., Rao, A.M.: Chem. Phys. Lett. **412**, 269–273 (2004)
100. Liang, E.J., Ding, P., Zhang, H.R., Guo, X.Y., Du, Z.L.: Diam. Relat. Mater. **13**, 69–73 (2004)
101. Wang, X.B., Liu, Y.Q., Zhang, L., Ma, H.Z., Yao, N., Zhang, B.L.: J. Phys. Chem. B **106**, 2186–2190 (2002)
102. Lee, C.J., Lyu, S.C., Kim, H.W., Lee, J.H., Cho, K.I.: Chem. Phys. Lett. **359**, 115–120 (2002)
103. Glerup, M., Castignolles, M., Holzinger, M., Hug, M., Loiseau, A., Bernier, P.: Chem. Commun. **20**, 2542–2543 (2003)
104. Jang, J.W., Lee, C.E., Lyu, S.C., Lee, T.J., Lee, C.J.: Appl. Phys. Lett. **84**, 2877–2879 (2004)
105. Lee, Y.T., Kim, N.S., Bae, S.Y., Park, J., Yu, S.C., Ryu, H.: J. Phys. Chem. B **107**, 12958–12963 (2003)
106. Koziol, K., Shaffer, M., Windle, A.: Adv Mater **17**, 760–763 (2005)
107. Friedrichs, S., Windle, A.H., Koziol, K., Ducati, C., Midgley, P.A.: Microsc. Microanal. **11**, 1536–1537 (2005)
108. Ducati, C., Koziol, K., Friedrichs, S., Yates, T.J.V., Shaffer, M.S., Midley, P.A., Windle, A. H.: Small **2**, 774–784 (2006)
109. Ducati, C., Koziol, K., Stavrinadis, A., Friedrichs, S., Windle, A.H., Midgley, P.A.: J. Phys. Conf. Ser. **26**, 199–202 (2006)
110. Ren, Z.F., Huang, Z.P., Xu, J.W., Wang, J.H., Bush, P., Siegal, M.P., Provencio, P.N.: Science **282**, 1105 (1998)
111. Qin, L.C., Zhou, D., Krauss, A.R., Gruen, D.M.: Appl. Phys. Lett. **72**, 3437 (1998)
112. Tsai, S.H., Chao, C.W., Lee, C.L., Shih, H.C.: Appl. Phys. Lett. **74**, 3462 (1999)
113. Choi, Y.C., Shin, Y.M., Lee, Y.H., Lee, B.S., Park, G.S., Choi, W.B., Lee, N.S., Kim, J.M.: Appl. Phys. Lett. **76**, 2367 (2000)
114. Bower, C., Zhu, W., Jin, S., Zhou, O.: Appl. Phys. Lett. **77**, 830 (2000)
115. Okai, M., Muneyoshi, T., Yaguchi, T., Sasaki, S.: Appl. Phys. Lett. **77**, 3468 (2000)
116. Merkulov, V.I., Lowndes, D.H., Wei, Y.Y., Eres, G., Voelkl, E.: Appl. Phys. Lett **76**, 1534 (2000)
117. Chhowalla, M., Teo, K.B.K., Ducati, C., Rupesinghe, N.L., Amaratunga, G.A.J., Ferrary, A. C., Roy, D., Robertson, J., Milne, W.I.: J. Appl. Phys. **90**, 5308 (2001)
118. Li, J., Stevens, R., Delzeit, L., Ng, H.T., Cassell, A., Han, J., Meyyappan, M.: Appl. Phys. Lett. **81**, 910 (2002)
119. Delzeit, L., McAninch, I., Cruden, B.A., Hash, D., Chen, B., Han, J., Meyyappan, M.: J. Appl. Phys. **91**, 6027 (2002)
120. Wang, Y.H., Lin, J., Huan, C.H.A., Chen, G.S.: Appl. Phys. Lett. **79**, 680 (2001)
121. Boskovic, B.O., Stolojan, V., Khan, R.U., Haq, S., Silva, S.R.P.: Nat. Mater. **1**, 165 (2002)

122. Lee, O.J., Lee, K.H.: Appl. Phys. Lett. **82**, 3770 (2003)
123. Teo, K.B.K., Chhowalla, M., Amaratunga, G.A.J., Hasko, D.G., Pirio, G., Legagneux, P., Wyczisk, F., Pribat, D.: Appl. Phys. Lett. **79**, 1534 (2001)
124. Minea, T.M., Point, S., Granier, A., Touzeau, M.: Appl. Phys. Lett. **85**, 1244 (2004)
125. Hofmann, S., Ducati, C., Kleinsorge, B., Robertson, J.: Appl. Phys. Lett. **83**, 135 (2003)
126. Hofmann, S., Ducati, C., Kleinsorge, B., Robertson, J.: Appl. Phys. Lett **83**, 4661 (2003)
127. Cantoro, M., Hofmann, S., Pisana, S., Scardaci, V., Parvez, A., Ducati, C., Ferrari, A.C., Blackburn, A.M., Wang, K.Y., Robertson, J.: Nano Lett. **6**, 1107 (2006)
128. Kasuya, D., Yudasaka, M., Takahashi, K., Kokai, F., Iijima, S.: J. Phys. Chem. B **106**, 4947 (2002)
129. Kawai, T., Miyamoto, Y., Sugino, O., Koga, Y.: Phys. Rev. B **66**, 033404 (2002)
130. Chen, C.C., Chen, C.F., Lee, I.H., Lin, C.L.: Diam. Relat. Mater. **14**, 1897 (2005)
131. Shang, N.G., Au, F.C.K., Meng, X.M., Lee, C.S., Bello, I., Lee, S.T.: Chem. Phys. Lett. **358**, 187 (2002)
132. Wang, J.J., Zhu, M.Y., Outlaw, R.A., Zhao, X., Manos, D.M., Holloway, B.C.: Carbon **42**, 2867 (2004)
133. Lin, C.H., Chang, H.L., Tsai, M.H., Kuo, C.T.: Diam. Relat. Mater. **11**, 922 (2002)
134. Du, J.M., Liu, Z.M., Li, Z.H., Han, B.X., Sun, Z.Y., Huang, Y.: Mater. Lett. **59**, 456 (2005)
135. Wu, Y.H., Qiao, P.W., Chong, T.C., Shen, Z.X.: Adv. Mater. **14**, 64 (2002)
136. Hiraki, H., Jiang, N., Wang, H.X., Hiraki, A.: J. Phys. IV. **132**, 111 (2006)
137. Nishimura, K., Jiang, N., Hiraki, A.: IEICE Trans. Electron. **E86C**, 821 (2003)
138. Chuang, A.T.H., Boskovic, B.O., Robertson, J.: Diam. Relat. Mater. **15**, 1103 (2006)
139. Chuang, A.T.H., Robertson, J., Boskovic, B.O., Koziol, K.K.K.: Appl. Phys. Lett. **90**, 123107 (2007)
140. Vigolo, B., Penicaud, A., Coulon, C., Sauder, C., Pailler, R., Journet, C., Bernier, P., Poulin, P.: Science **290**, 1331 (2000)
141. Somoza, A.M., Sagui, C., Roland, C.: Phys. Rev. B **63**, 081403 (2001)
142. Song, W., Kinloch, I.A., Windle, A.H.: Science **302**, 1363 (2003)
143. Nikolaev, P., Bronikowski, M.L., Bradley, R.K., Rohmund, F., Colbert, D.T., Smith, K.A., Smalley, R.E.: Chem. Phys. Lett. **313**, 91 (1999)
144. Bronikowski, M.J., Willis, P.A., Colbert, D.T., Smith, K.A., Smalley, R.E.: J. Vac. Sci. Technol. A Vac. Surf. Films **19**, 1800 (2001)
145. Ramesh, S., Ericson, L.M., Davis, V.A., Saini, R.K., Kittrell, C., Pasquali, M., Billups, W.E., Adams, W.W., Hauge, R.H., Smalley, R.E.: J. Phys. Chem. B **108**, 8794 (2004)
146. Ericson, L.M., Fan, H., Peng, H., Davis, V.A., Zhou, W., Sulpizio, J., Wang, Y., Booker, R., Vavro, J., Guthy, C., Nicholas, A., Parra-Vasquez, G., Kim, M.J., Ramesh, S., Saini, R.K., Kittrell, C., Lavin, G., Schmidt, H., Adams, W.W., Billups, W.E., Pasquali, M., Hwang, W. F., Hauge, R.H., Fischer, J.E., Smalley, R.E.: Science **305**, 1447 (2004)
147. Zhang, S., Koziol, K.K.K., Kinloch, I.A., Windle, A.H.: Small **4**, 1217–1222 (2008)
148. Jiang, K., Li, Q., Fan, S.: Nature **419**, 801 (2002)
149. Zhang, M., Atkinson, K.R., Baughman, R.H.: Science **306**, 1358 (2004)
150. Zhang, M., Fang, S., Zakhidov, A.A., Lee, S.B., Aliev, A.E., Williams, C.D., Atkinson, K.R., Baughman, R.H.: Science **309**, 1215 (2005)
151. Zhang, X., Li, Q., Tu, Y., Li, Y., Coulter, J.Y., Zheng, L., Zhao, Y., Jia, Q., Peterson, D.E., Zhu, Y.: Small **3**, 244–248 (2007)
152. Li, Y.L., Kinloch, I.A., Windle, A.H.: Science **304**, 276 (2004)
153. Koziol, K., Vilatela, J., Moisala, A., Motta, M., Cunniff, P., Sennett, M., Windle, A.: Science **318**, 1892–1895 (2007)
154. Baughman, R.H., Zakhidov, A.A., de Heer, W.A.: Science **297**, 787 (2002)
155. Tennent, H., Hausslein, R.W., Leventis, N., Moy, D.: Hyperion Catalysis International, Inc. Patent US 5,846,658, 8 December 1998
156. Downs, W.B., Baker, R.T.K.: Carbon **29**, 1173 (1991)
157. Downs, W.B., Baker, R.T.K.: J. Mater. Res. **10**, 625 (1995)

158. Thostenson, E.T., Li, W.Z., Wang, D.Z., Ren, Z.F., Chou, T.W.: J. Appl. Phys. **91**, 6034 (2002)
159. Sun, X., Li, R., Villers, D., Dodelet, J.P., Desilets, S.: Chem. Phys. Lett. **379**, 99 (2003)
160. Wang, C., Waje, M., Wang, X., Tang, J., Haddon, R.C., Yan, Y.: Nano Lett. **4**, 345 (2004)
161. Marphy, M.A., Wilcox, G.D., Dahm, R.H., Marken, F.: Electrochem. Commun. **5**, 51 (2003)
162. Jo, S.H., Wang, D.Z., Huang, J.Y., Li, W.Z., Kempa, K., Ren, Z.F.: Appl. Phys. Lett. **85**, 810 (2004)
163. Boskovic, B.O., Golovko, V., Cantoro, M., Kleinsorge, B., Ducati, C., Chuang, A.T.H., Hofmann, S., Robertson, J., Johnson, B.F.G.: Carbon **43**, 2643 (2005)
164. Hart, A.J., Boskovic, B.O., Chuang, A.T.H., Golovko, V.B., Robertson, J., Johnson, B.F.G., Slocum, A.H.: Nanotechnology **17**, 1397 (2006)
165. Boskovic, B.O.: The Morgan Crucible Company Plc. Synthesis of carbon nanotubes and/or nanofibres on a porous fibrous matrix. WO 2004078649, 16 September 2004
166. Veedu, V.P., Cao, A., Li, X., Ma, K., Soldano, C., Kar, S., Ajayan, P.M., Ghasemi-Nejhad, M.N.: Nat. Mater. **5**, 458 (2006)
167. Boskovic, B.O.: Meggitt Aerospace Ltd. Carbon-carbon composite. Patent Int. Pub. No. WO 2009/004346 A1, 7 March 2007

http://www.springer.com/978-3-642-14672-5

Carbon and Oxide Nanostructures
Synthesis, Characterisation and Applications
Yahya, N.
2011, VIII, 416 p., Hardcover
ISBN: 978-3-642-14672-5